Applied Catalysis B: Environmental 163 (2015) 30–39

Contents lists available at ScienceDirect

Applied Catalysis B: Environmental

journal homepage: www.elsevier.com/locate/apcatb

Promotional effect of vanadium on the selective catalytic oxidation of NH_3 to N_2 over $Ce/V/TiO_2$ catalyst

Sang Moon Lee, Sung Chang Hong*

Department of Environmental Energy Engineering, Graduate School of Kyonggi University, 94-6 San, Iui-dong, Youngtong-ku, Suwon-si, Gyeonggi-do 442-760, Republic of Korea

ARTICLE INFO

Article history:
Received 29 April 2014
Received in revised form 25 June 2014
Accepted 21 July 2014
Available online 27 July 2014

Keywords:
Ce/TiO_2 catalyst
Vanadium
NH_3
Selective catalytic oxidation
SO_2

ABSTRACT

The promotional effect of vanadium on Ce/TiO_2 catalyst for the selective catalytic oxidation of NH_3 to N_2 was investigated. The catalytic activity and SO_2 tolerance of 10 wt% Ce/TiO_2 catalyst were greatly enhanced by the addition of 2 wt% vanadium, in the temperature range of 250–350 °C. The NH_3 conversion of 10 wt% Ce/TiO_2 had been highly enhanced from 50 to 90% at 300 °C, after vanadium addition. The BET and XPS results indicated that the addition of vanadium could result in better dispersion of Ce^{4+} species on TiO_2, leading to the enhancement of BET surface area. H_2 temperature programmed reduction (TPR) results suggest that vanadium enhances the redox properties, and the absence of bulk CeO_2 in high temperature (700 °C) peak indicates it could be attributed to the strong interactions among CeO_x, VO_x, and TiO_x. More importantly, 10 wt% Ce/2 wt% V/TiO_2 catalyst showed strong resistance to SO_2 poisoning. DRIFT results suggest that the 10 wt% Ce/2 wt% V/TiO_2 catalyst could reduce the formation of NH_4HSO_4 species, which was beneficial for easy decomposition, in the presence of SO_2. In summary, these results indicated that the 10 wt% Ce/2 wt% V/TiO_2 catalyst greatly improved SCO activity and SO_2 tolerance.

1. Introduction

Ammonia (NH_3) emission from stationary and mobile sources has remained a very important issue as an environmental problem, and for human health. NH_3 removal technologies are required in various industries, such as chemical process, industrial wastewater, semiconductor manufacture process, and downstream of NO_x system removal, etc. Among the NH_3 removal technologies, the selective catalytic oxidation (SCO) of NH_3 to N_2 is potentially an attractive technology. In recent years, many studies have focused on the SCO catalysts. Many noble metal oxide catalysts, such as $Pt/CuO/Al_2O_3$ [1], RuO_2 [2], $Au/CeO_2/Al_2O_3$ [3], Pd/Al_2O_3 [4], and Ag/Al_2O_3 [5], have been investigated over the past several decades. Among these catalysts, Pt based catalyst have been found to be highly active and selective for the oxidation of NH_3 to N_2. However, Pt based catalyst is only efficient within a narrow temperature window of 180–220 °C. Many transition-metal-oxide catalysts, such as CuO [6], Fe_2O_3 [7], CoO_3 [8], MoO_3 [9], MnO_2 [10], and CeO_2 [11], have also been reported, and are thought to be promising alternatives to the noble metal based catalysts. Among them, cerium-oxide-based catalysts, such as $Ce\text{-}TiO_2$ [12], $CeO_2\text{-}Al_2O_3$ [13], $Ce\text{-}WO_3\text{-}TiO_2$ [14], $CeO_2\text{-}TiO_2\text{-}SiO_2$ [15], and $Mn\text{-}CeO_2\text{-}TiO_2$ [16] have been found to have high activity on selective catalytic reduction (SCR) of NO by NH_3, due to their high oxygen storage capacity, many oxygen vacancies, strong interactions with metals, and ability to easily convert between Ce^{3+} and Ce^{4+} [17,18]. Recently, ceria-based catalysts were also investigated for the selective catalytic oxidation reaction of NH_3 to N_2. Wang et al. [11] found that the $CeO_2\text{-}ZnO_2$ mixed catalysts showed high NH_3 oxidation activity at 360 °C; and Wang et al. [14] investigated a $CuO–CeO_2$ mixed catalyst that exhibited the highest NH_3 conversion at 250 °C. In our previous study, we have found that the 10 wt% Ce/TiO_2 catalyst calcined at 400 °C had high SCO activity, in the temperature range of 300–350 °C [19]. Since diesel fired exhausts and flue gas after desulfurization contain low concentrations of residual SO_2, understanding the effects of SO_2 on SCO activity is important, for the development and application of appropriate catalysts [20]. Many efforts have been made to develop sulfur resistant catalysts for low temperature SCR [21–23]. However, there has been no report of an investigation that focuses on the increasing catalytic activity and SO_2 tolerance of the Ce/TiO_2 catalyst in the SCO reaction. Therefore, in the present study, we focused on the physical chemistry characteristics, and the SO_2 tolerance for Ce/TiO_2 catalyst, prepared by the addition of vanadium. The catalysts were then characterized, using Brunauer-Emmett-Teller (BET), X-ray diffraction (XRD), temperature-programmed reduction (TPR) of H_2, X-ray

* Corresponding author. Tel.: +82 31 249 9744; fax: +82 31 254 4905.
E-mail address: schong@kyonggi.ac.kr (S.C. Hong).

http://dx.doi.org/10.1016/j.apcatb.2014.07.043
0926-3373/

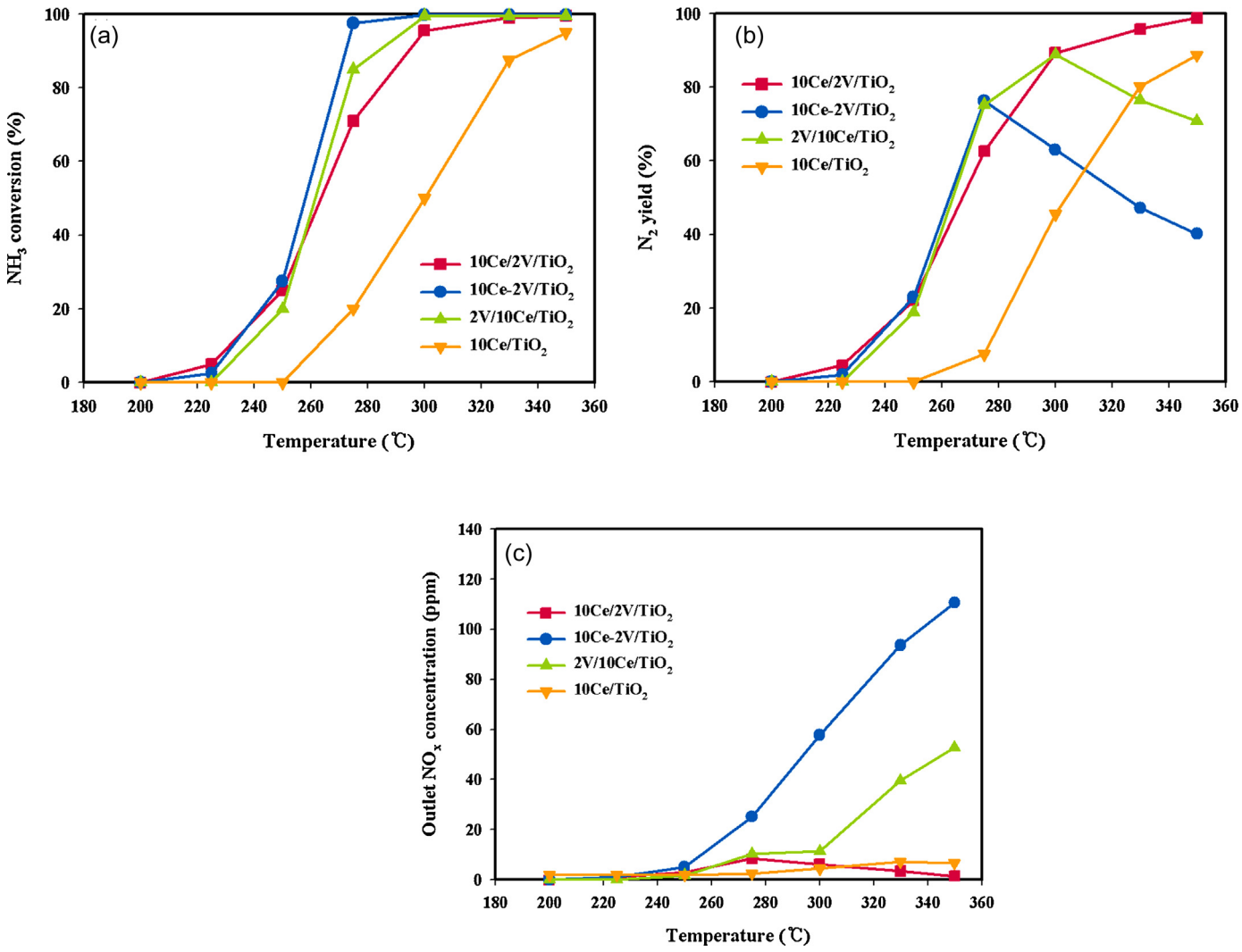

Fig. 1. NH_3 oxidation activities of $10Ce/TiO_2$, $10Ce/2V/TiO_2$, $10Ce\text{-}2V/TiO_2$, $2V/10Ce/TiO_2$ and $10Ce/TiO_2$ catalysts: (a) NH_3 conversion, (b) N_2 yield, and (c) outlet NO_x concentration.

photoelectron spectroscopy (XPS), and Fourier-transform infrared (FT-IR) spectroscopy, to obtain knowledge about their activity and SO_2 tolerance in the SCR process.

2. Experimental

2.1. Catalyst preparation

All of the V doped Ce/TiO_2 catalysts were prepared by a wet impregnation method, using G-5 support, which is a commercial anatase TiO_2 supplied by Cristal Global Co. For 2 wt% V/TiO_2 catalyst, ammonium metavanadate [NH_4VO_3; Aldrich Chemical Co.] were dissolved in distilled water at 80 °C; in order to increase the solubility of ammonium metavanadate, oxalic acid was added little-by-little while stirring, until the pH became 2.5. This solution was made by adding TiO_2 support, stirred for 30 min, then moisture was evaporated at 70 °C using a rotary vacuum evaporator, and the products were then dried at 110 °C overnight. The catalysts were calcined, ranging from 400 °C for 4 h. For 10 wt% Ce/TiO_2 catalyst, cerium nitrate hydrate [$Ce(NO_3)_3{\cdot}6H_2O$; Aldrich Chemical Co.] were dissolved in distilled water at 80 °C. This solution was made by adding TiO_2 support which was as the same method as that mentioned above. 10 wt% Ce-2 wt%V/TiO_2 catalyst was prepared by co-impregnation of ammonium metavanadate and cerium nitrate hydrate solutions and TiO_2 support, which was as the same method as that mentioned above. 2 wt%V/10 wt% Ce/TiO_2 catalyst was prepared by impregnation of ammonium metavanadate solution and Ce/TiO_2 support, which was as the same method as that mentioned above. And 10 wt% Ce/X wt%V/TiO_2 catalysts were also prepared by impregnation of cerium nitrate hydrate solution and V/TiO_2 support, which was as the same method as that mentioned above. The vanadium oxide content in 10 wt% Ce/X wt%V/TiO_2 catalyst was 1% 1.5% and 2% by weight, respectively. All the above catalysts were ground, and sieved through 40–50 mesh. The sulfated catalysts were obtained by exposing the catalyst to a 200 ppm SO_2 stream at each reaction temperature for 5 h. The following is an example of the notation used to refer to the prepared catalysts: $10Ce/2V/TiO_2$, $10Ce\text{-}2V/TiO_2$, and $2V/10Ce/TiO_2$ denotes 10 wt% Ce/2 wt% V/TiO_2, 10 wt% Ce-2 wt% V/TiO_2, and 2 wt% V/10 wt% Ce/TiO_2.

2.2. Characterizations

The surface areas of the ceria based catalyst powders were measured via physical nitrogen adsorption at −196 °C, using an ASAP 2010 (Micrometrics). The specific surface area was analyzed using the Brunauer-Emmett-Teller (BET) model, with 0.3 g samples of the catalysts being degassed at 300 °C for 2 h. X-ray diffraction measurements were carried out, using Cu Kα

(λ = 1.5056 Å) radiation. The catalysts were run at 2θ = 20–90°, with a step size of 0.1° and time step of 1.0 s, using an X'Pert PRO MRD (PANalytical). The temperature-programmed reduction of H_2 was measured under 10% H_2/Ar, using 0.3 g samples of the catalysts, at a total flow rate of 50 cc/min. Before the H_2 TPR measurements, the catalysts were pretreated in a flow of 5% O_2/Ar at 300 °C for 0.5 h, then cooled to 50 °C. Each catalyst sample was placed in dilute hydrogen, and the consumption of hydrogen was monitored using Autochem 2920 (Micrometrics), while the temperature was increased to 800 °C, at a rate of 10 °C/min. X-Ray photoelectron spectroscopy analysis was performed, using an ESCALAB 210 instrument (VG Scientific), with monochromatic Al Kα (1486.6 eV) as the excitation source. The samples were dried at 100 °C for 24 h, and then analyzed without surface sputtering and etching, in order to maintain the vacuum pressure of the XPS equipment of 10^{-6} Pa. The binding energies and intensities of the Ce 3d, V2p, Ti 2p, O 1s, and C 1s signals in the specimens were analyzed, based on wide-scanning spectra. Sample charge effects were eliminated, by correcting the observed spectra, using the C 1s binding energy (BE) value of 284.6 eV. Fourier-transform infrared spectroscopy experiments were conducted in a diffuse reflection cell equipped with a CaF_2 window, using a 660 plus FT-IR spectrometer (JASCO). The spectra included 30 accumulated scans at a resolution of 4 cm^{-1}, using a mercury-cadmium-telluride (MCT) detector. Prior to the measurements, the catalyst samples were pretreated in Ar at 400 °C for 1 h. Then, a gas mixture comprising 0.5% NO/Ar and 0.5% NH_3/Ar + 8% O_2 in Ar (100 cc/min) or 0.1% SO_2/Ar + 8% O_2 in Ar (100 cc/min) was passed through the sample. After a steady-state was reached, the FT-IR spectra were recorded.

2.3. Catalytic activity tests

The SCO apparatus consisted of a continuous-flow-type fixed-bed reaction system that comprised a quartz tube (inner diameter: 8 mm; height: 650 mm), and a catalytic bed that was fixed, using quartz wool. The catalyst samples were made using a hydraulic press with 5000 pounds of force to produce pellets, and 40–50 mesh sieve; they were then charged into a quartz tube. The temperature of the reactor was controlled, using a PID controller and a K-type thermocouple that was fixed on the bottom of the bed. To measure the gas inlet temperature, another K-type thermocouple was installed at the top of the catalytic bed. The feed gases comprised 200 ppm NH_3, 8% O_2, 6% moisture, and 200 ppm SO_2 (when used). The total flow through the reactor was 500 cm^{-3}/min, and a gas hourly space velocity of 60,000 and 120,000 h^{-1} was obtained. The premixed gases were supplied by a mass flow controller (MKS). Moisture was added to the reactor, by injecting N_2 containing water vapor through the bubbler; the moisture level was kept constant, by circulating water at a fixed temperature of 45 °C, using a circulator outside the jacket-type bubbler. The entire gas-supply pipe was made of stainless steel, and wrapped with a heating band set at 180 °C, to prevent condensation. Before the catalytic activity test, the sample was pretreated in a flow of 8% O_2/N_2 at 400 °C for 0.5 h. The concentrations of the reactants and products were measured as follows: The inlet and outlet NO concentrations were determined using a NO_x analyzer (Fuji Electric Global), and N_2O concentrations were analyzed using an N_2O analyzer (Ultramat 6; Siemens), while the concentration of SO_2 was monitored by a SO_2 analyzer (Thermo, Model 43 C). The concentrations of NO_2 and NH_3 were measured using different detector tubes: 9L, 3M, 3La and 3L (Gastec Co.). When the SCO reaction reached a steady-state, the NH_3 conversion and N_2 yield were calculated from the concentrations of the gases, according to equations (1) and (2).

$$NH_3\ \text{conversion}\,(\%) = \left(\frac{[NH_3]_{in} - [NH_3]_{out}}{[NH_3]_{in}}\right) \times 100 \quad (1)$$

$$N_2\ \text{yield}\,(\%) = \left(\frac{[NH_3]_{in} - [NH_3]_{out} - [NO]_{out} - [NO_2]_{out} - 2[N_2O]_{out}}{[NH_3]_{in}} \times 100\right) \quad (2)$$

3. Results and discussion

3.1. Catalytic activity

In preparation of a ternary catalyst, the preparation method and mixing order of active metal and support is very important for the catalytic activity. They can highly affect the binding structure, valence state, and dispersion of metal oxides, and redox properties. Fig. 1 shows the NH_3 conversion, N_2 yield, and outlet NO_x concentration of the Ce/Ti, Ce/V/Ti, Ce-V/Ti, and V/Ce/Ti catalysts via appropriate amount of 10 wt% Ce and 2 wt% V, for SCO reaction at a gases space velocity of 60,000 h^{-1}. As shown in Fig. 1(A), the NH_3 conversion at 275–350 °C decreased, as follows: 10Ce-2V/TiO_2 > 2V/10Ce/TiO_2 > 10Ce/2V/TiO_2 > 10Ce/TiO_2. NH_3 removal efficiency must be considered for the NH_3 conversion rate, as well as N_2 yield and outlet NO_x concentration, because ammonia could convert into N_2 and NO_x in the SCO reaction. So, we evaluated the N_2 yield and outlet NO_x concentration of all catalysts. In Fig. 1(b) and (c), the 10Ce/TiO_2 catalyst showed an 80% N_2 yield, and NO_x was not detected. However, it showed a low catalytic activity, which achieved 80% conversion of NH_3 at 300 °C. Meanwhile, 10Ce/2V/TiO_2 catalyst showed a 90% N_2 yield, and a low concentration of NO_x (<10 ppm) was formed. Although 2V/10Ce/TiO_2 and 10Ce-2V/TiO_2 catalysts enabled high NH_3 conversion at temperatures ranging from 300 to 350 °C, the N_2 yield significantly decreased, and the NO_x were formed at above 300 °C. This may be attributed to the strong oxidation ability of vanadium as active sites [24]. This result indicates that the addition of vanadium and mixing order have significantly effects for SCO reaction over Ce/TiO_2 catalyst, in the temperature of 275–350 °C. Among these catalysts, 10Ce/2V/TiO_2 prepared by an impregnation method showed the highest NH_3 conversion to N_2, above 96% of NH_3 conversion, and 90% of N_2 yield, at the temperature of 300 °C.

The effects of various vanadium loadings (0, 1, 1.5, 2 wt%) on the SCO activity of 10Ce/X wt%V/TiO_2 catalyst are shown in Fig. 2. Fig. 2(a) shows the NH_3 conversion over 10Ce/X wt%V/TiO_2 catalysts within the temperature range of 200–350 °C. As expected, at a relatively high gas hourly space velocity (GHSV) of 120,000 h^{-1}, the activity of 10Ce/TiO_2 catalyst exhibited low NH_3 conversion, revealing only about 50% NH_3 conversion at 300 °C, in our previous studies [19]. As the vanadium loading increased, the NH_3 conversion sequentially increased, within the entire temperature range. The NH_3 conversion activity was greatly improved from 50% to 90% at 300 °C on 10Ce/TiO_2 catalyst, by 2 wt% vanadium addition. However, the addition of 3% vanadium to the 10Ce/TiO_2 catalyst could not increase the SCO activity, which showed a very similar trend on 10Ce/1.5 V/TiO_2 catalyst (not shown). Furthermore, high amount of vanadium as catalyst is harmful to environmental aspect. Therefore, it is not necessary to investigate the effect of the 10Ce/3 V/TiO_2 catalyst in this study. The vanadium loading has a strong effect on the N_2 yield and outlet NO_x concentration, and showed a similar trend to the NH_3 conversion; as the vanadium loading increased up to 2 wt% vanadium, the N_2 yield sequentially increased within the entire temperature range, and small amounts of NO_x were formed below 20 ppm, within the entire temperature range. In the experiment results of the vanadium impregnation sequence and loadings, we could find that a promotional effect was obtained, when vanadium was modified over 10CeO_2/TiO_2 catalyst, and the 10Ce/2V/TiO_2 catalyst had the best activity for the SCO reaction.

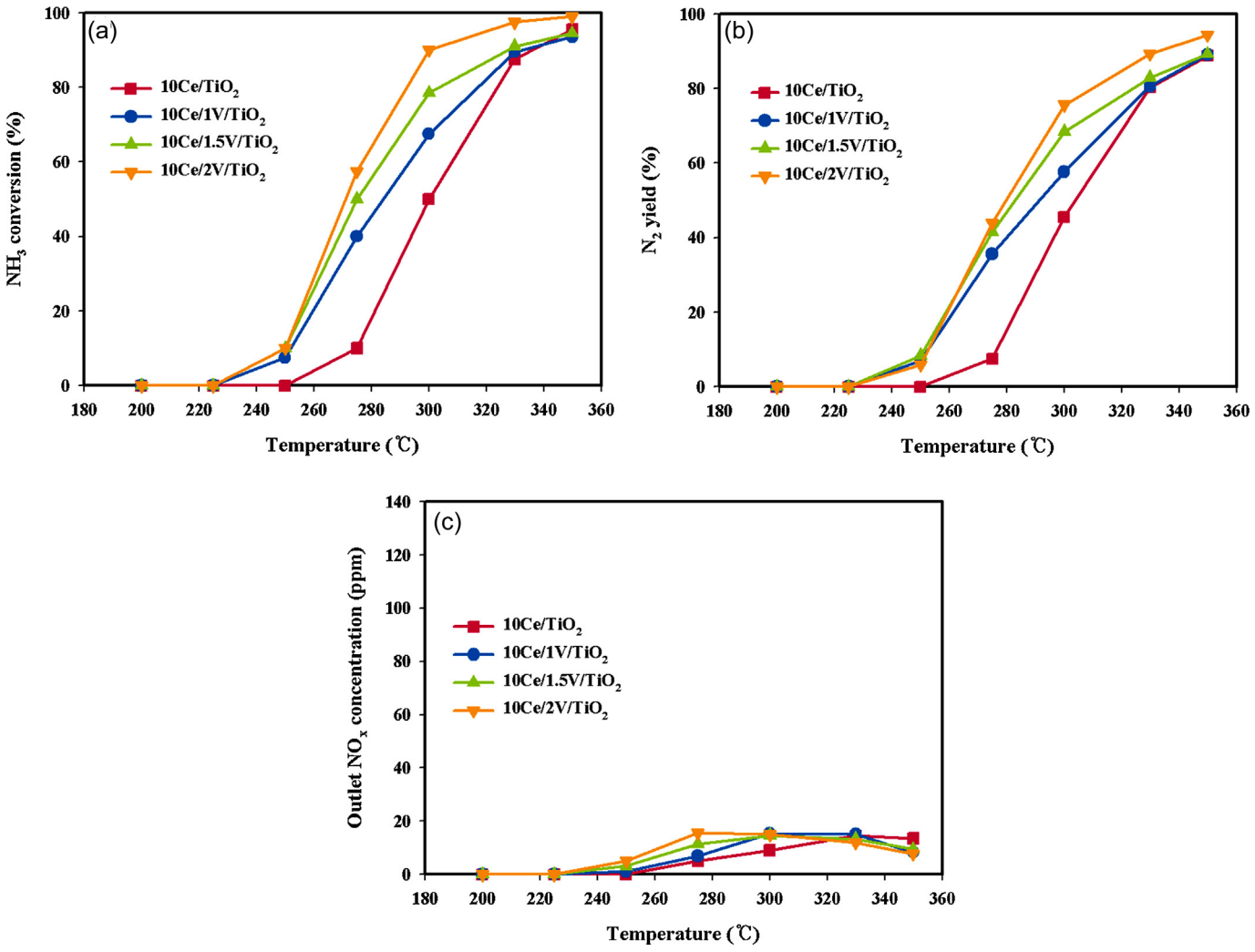

Fig. 2. NH_3 oxidation activities of 10Ce/X wt%V/TiO_2 catalysts with vanadium loadings: (a) NH_3 conversion, (b) N_2 yield, and (c) outlet NO_x concentration.

3.2. Catalyst characterization

3.2.1. Physical properties of Ce/TiO_2 and Ce/V/TiO_2 catalysts

To confirm the vanadium effect of the 10Ce/2V/TiO_2 catalyst, various characteristic analysts were carried out for 10Ce/TiO_2 and 10Ce/2V/TiO_2 catalysts. Firstly, X-ray diffraction (XRD) was used to analyze the crystal structure of TiO_2, 10Ce/TiO_2 and 10Ce/X wt%V/TiO_2 catalysts, as shown in Fig. 3. XRD patterns obtained from TiO_2 sample is also shown, for comparison. For pure TiO_2, the main peaks were observed at 25.3, 37.1 and 47.5°, which have been investigated in our previous studies [19]. For 10Ce/TiO_2 and 10Ce/2V/TiO_2 catalysts, the CeO_2 peaks were not found in the XRD results, and typically, anatase TiO_2 peaks could only be observed at 25.3, 37.1, and 47.5°. It is noteworthy that the ceria oxides were well dispersed on the TiO_2 support structure, and that they were in amorphous state. It is well known that the major peaks of the two vanadium oxide phases principally identify at 28°, 37° and 55° for the VO_2, and at 20°, 26° and 31° for the V_2O_5 [25]. For 10Ce/2V/TiO_2 catalysts, no crystalline phase corresponding to vanadium oxides peaks was detected, and the intensity of the TiO_2 peaks was increased, which is most likely due to the amorphous state of vanadium oxide, and the strong background from TiO_2. It has been reported that vanadium can incorporate into the anatase TiO_2 [26].

The BET surface area, pore volume, and average pore diameter of the TiO_2, 10Ce/TiO_2 and 10Ce/2V/TiO_2 catalysts are shown in Table 1. The addition of a vanadium metal to the 10Ce/TiO_2 catalyst apparently increased the surface area from 74.485 to 104.24 m^2/g.

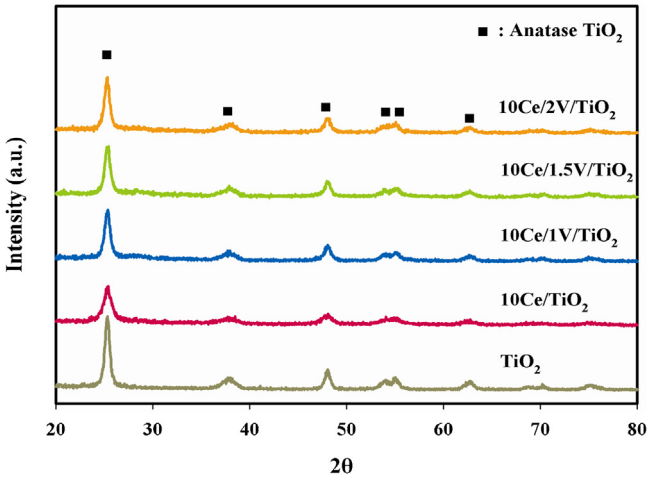

Fig. 3. XRD patterns of TiO_2 and 10Ce/X wt%V/TiO_2 catalysts with vanadium loadings.

Table 1
The surface area, total pore volume and average pore diameter of the 10Ce/TiO_2 and 10Ce/2V/TiO_2 catalysts.

Catalyst	BET surface area (m^2/g)	Total pore volume (cm^3/g)	Average pore diameter (nm)
TiO_2	136.5	0.4491	13.159
10Ce/TiO_2	74.48	0.5254	28.215
10Ce/2V/TiO_2	104.24	0.3550	13.624

In contrast, the average pore diameter and total pore volume decreased from 28.215 to 13.624 nm, and 0.5254 to 0.355 cm^3/g, respectively, as expected. These results indicated that the surface area of the 10Ce/2V/TiO_2 catalyst is highly enhanced, due to the formation of small pores; and the catalyst would keep more space between the particles, and avoid the collapse of microspores [27]. The addition of vanadium metal can change the surface structure of the 10Ce/TiO_2 catalyst, which is in agreement with previously reported studies over the addition of metal in Mn/TiO_2 catalyst [16].

3.2.2. H_2-TPR analysis

To investigate the effect of vanadium doping on the reducibility of the catalysts, H_2-temperature programmed reduction (TPR) experiments were performed. Fig. 4 shows the H_2 TPR profiles of the pure CeO_2, TiO_2, 2V/TiO_2, 10Ce/TiO_2 and 10Ce/2V/TiO_2 catalysts. The maximum reduction peak of TiO_2 exhibited at 485 °C, and CeO_2 exhibited two broad peaks at about 460 and 750 °C, which can be assigned to the reduction of surface oxygen and lattice oxygen, respectively [19]. The TPR profiles of CeO_2 indicate that this material itself is not reducible, even at high temperatures [28,29]. The maximum reduction peak of 2V/TiO_2 catalyst exhibited at 350 °C. This reduction temperature is lower than that obtained for TiO_2 support [30]. It is likely to be a V-O-Ti interaction when the vanadium species are covered with TiO_2 surface. The 10Ce/TiO_2 catalyst shows three different reduction peaks at 410, 470 and 520 °C, which has been investigated in our previous studies [19]. The first peak at 410 °C was attributed to reduction of the surface oxygen of stoichiometric ceria (Ce^{4+}–O–Ce^{4+}) [31], and the second peak at 470 °C was attributed to reduction of nonstoichiometric ceria (Ce^{3+}–O–Ce^{4+}) [32]. The third peak at 520 °C was attributed to the reduction of bulk TiO_2 (Ti^{4+} to Ti^{3+}). This result concludes that the reduction with oxygen was enhanced by Ce, and was impregnated into the TiO_2 support, and high oxygen mobility is an important factor in the SCO reaction. In 10Ce/2V/TiO_2 catalyst, it showed the clear shift to lower ceria reduction temperature. An addition of vanadium to the 10Ce/TiO_2 catalyst showed only two distinct maximum peaks, at 380 and 435 °C. The first reduction peak of the surface oxygen of stoichiometric ceria (Ce^{4+}–O–Ce^{4+}) is significantly shifted from 410 °C to 380 °C. The second reduction peak of the surface oxygen of stoichiometric ceria (Ce^{3+}–O–Ce^{4+}) is significantly shifted from 480 °C to 435 °C. However, the third bulk TiO_2 reduction peak was not observed for 10Ce/2V/TiO_2 catalyst. This absence of the high-temperature (515 °C) peak indicates that the addition of vanadium would strengthen the V–O–Ti interactions, which makes it more difficult for the reduction of TiO_2 oxygen. Furthermore, the reduction peak of 2V/TiO_2 catalyst appeared at 350 °C was not observed for 10Ce/2V/TiO_2 catalyst. This could be attributed to the strong interaction between vanadium and titania during the additional calcination process for Ce impregnated 2V/TiO_2 catalyst. This strong interaction may be hard to oxygen mobility in V–O–Ti bonding. This strong interaction between V and Ti originates from the stabilization of V cations in the titania surface due to the remarkably close radius ratio (V:Ti = 0.063 nm:0.068 nm) [33]. However, V doping could improve the mobility of oxygen in ceria oxide. These results indicated that vanadium has preferentially strong interaction with the surface of the TiO_2 during first calcination process, indicating a decrease of the interaction between the ceria and calcined 2V/TiO_2 catalyst. Based on the reduction temperature and H_2 consumption amount, the introduction of vanadium would make the reduction of Ce^{4+}–O–Ce^{4+} species easier, and enhance the dispersion of active metal as Ce^{4+}–O–Ce^{4+} species. Gu et al. [27] reported that the addition of Ca into MnO_x-TiO_2 catalyst greatly enhanced the SCR activity, because strong interactions between Ca-Mn-Ti mixed complex would inhibit the sintering of MnOx and titania during the calcination process, thereby enhancing the surface area, oxygen mobility, and the dispersion of active phase. In the case of 10Ce/TiO_2 catalyst, the interactions between Ce and TiO_2 significantly influence the catalyst reducibility, and are largely dependent on the calcination temperature, which was confirmed in our previous study [19]. In brief, the addition of 2 wt% vanadium into 10Ce/TiO_2 catalyst greatly enhanced both the oxygen mobility, and the Ce dispersion, which was beneficial to the SCO reaction.

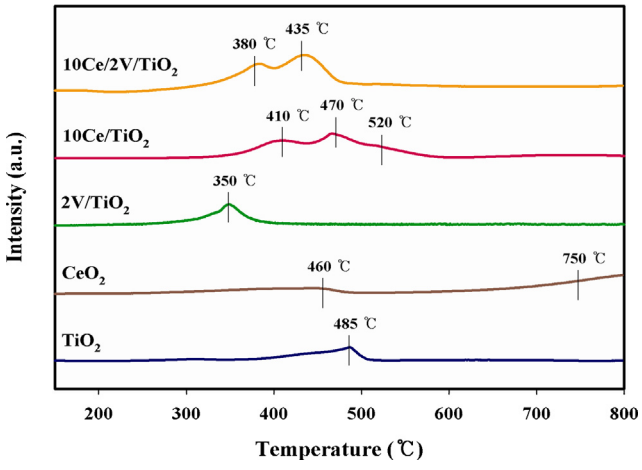

Fig. 4. H_2 TPR profiles of TiO_2, 10Ce/TiO_2 and 10Ce/2V/TiO_2 catalysts.

3.2.3. XPS analysis

10Ce/TiO_2 and 10Ce/2V/TiO_2 catalysts were investigated by XPS, to understand the surface atomic concentration and oxidation states of Ce on each catalyst. The Gaussian fitting results of Ce 3d spectrums are shown in Fig. 5(a). The complex peaks of the Ce 3d spectra were deconvoluted into eight peaks: The peaks referred to as u, u″, and u‴ were assigned to Ce^{4+} $3d_{3/2}$, and the peaks referred to as v, v″, and v‴ were assigned to Ce^{4+} $3d_{5/2}$. Peaks u′ and v′, which refer to $3d_{3/2}$ and $3d_{5/2}$, respectively, were contributed by the Ce^{3+} 3d final state [34]. The deconvoluted Ce 3d peaks with binding energies of 882.6, 890.5, 899.5, 902.2, 910.2, and 917.3 eV are attributed to Ce^{4+} species; and binding energies of 886.9, and 905.6 eV are attributed to Ce^{3+} species [35]. After vanadium addition, no shift in binding energy of the Ce 3d peak toward lower or higher binding energy was observed. Our previous XPS studies clearly indicate that the Ce^{4+} oxide was the main form of Ce in the catalysts with lower calcination temperature, which was beneficial to the SCO reaction. The surface atomic concentrations and surface molar percentages of ceria oxidation state are summarized in Table 2. The Ce^{4+} ratio, calculated by $Ce^{4+}/(Ce^{4+}+Ce^{3+})$, was apparently increased from 0.42 to 0.62 by the addition of 2 wt% vanadium. The atomic ratios of Ce/Ti over the surface of 10Ce/TiO_2 and 10Ce/2V/TiO_2 catalysts are 0.22 and 0.45. This result indicated that the addition of 2 wt% vanadium significantly improved the dispersion of the active ceria species over the surface of the catalyst, indicating that the V/TiO_2 support had better ceria oxide dispersion than the TiO_2 support, and enhanced the number of active sites per unit area for the SCO reaction. This result was consistent with the previous H_2-TPR result. Fig. 5(b) shows the binding energies of Ti 2p peaks for Ti $2p_{1/2}$ and Ti

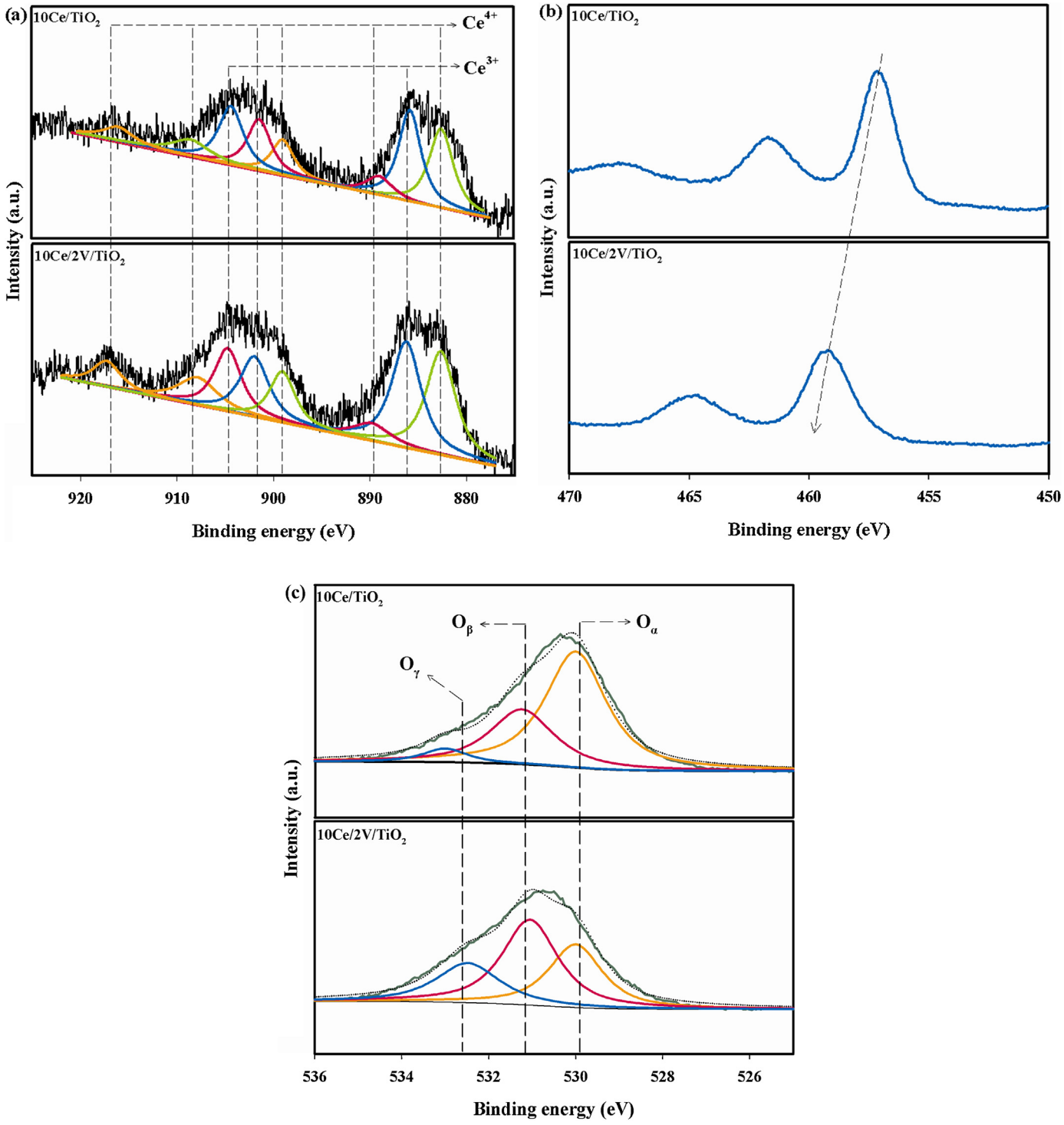

Fig. 5. XPS spectra of $10Ce/TiO_2$ and $10Ce/2V/TiO_2$ catalysts: (a) Ce 3d, (b) Ti 2p and (c) O 1s.

Table 2
The surface atomic concentration and surface molar percent of Ce 3d for $10Ce/TiO_2$ and $10Ce/2V/TiO_2$ catalysts.

Catalyst	Surface atomic concentration (%)				Surface molar percent of Ce 3d (%)
	Ce	V	Ti	Ce/Ti	$Ce^{4+}/(Ce^{3+}+Ce^{4+})$
$10Ce/TiO_2$	1.42	–	25.12	0.06	61.2
$10Ce/2V/TiO_2$	1.56	2.56	15.43	0.10	63.9

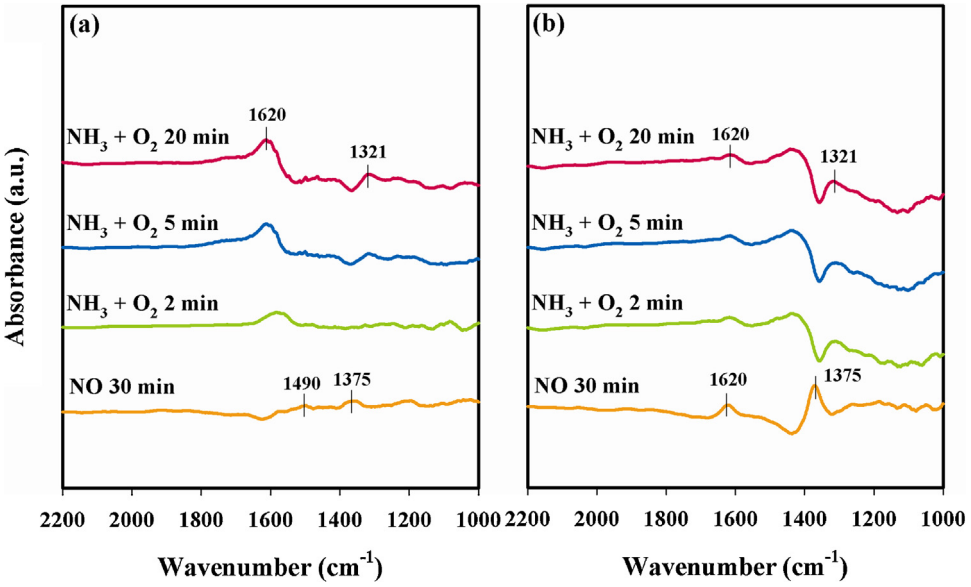

Fig. 6. DRIFT spectra of pre-adsorbed NO reacted with $NH_3 + O_2$ adsorption at 300 °C: (a) 10Ce/TiO_2, (b) 10Ce/2V/TiO_2.

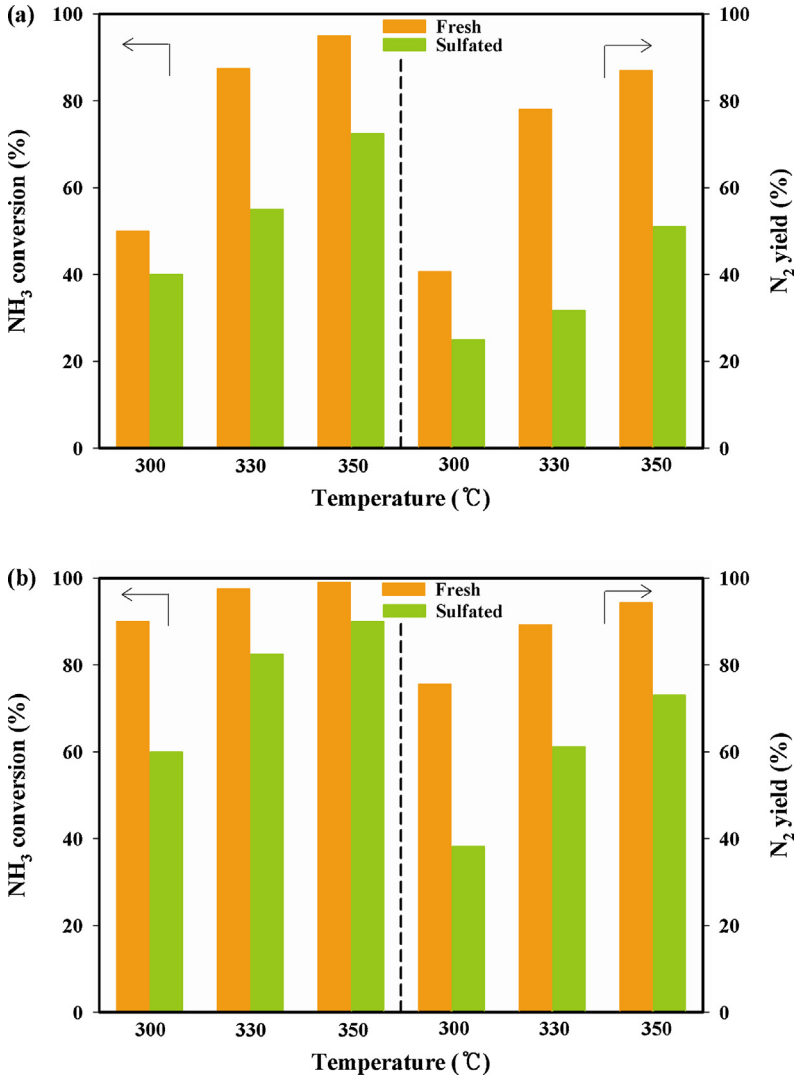

Fig. 7. NH_3 conversion and N_2 yield of fresh and sulfated catalysts: (a) 10Ce/TiO_2, (b) 10Ce/2V/TiO_2.

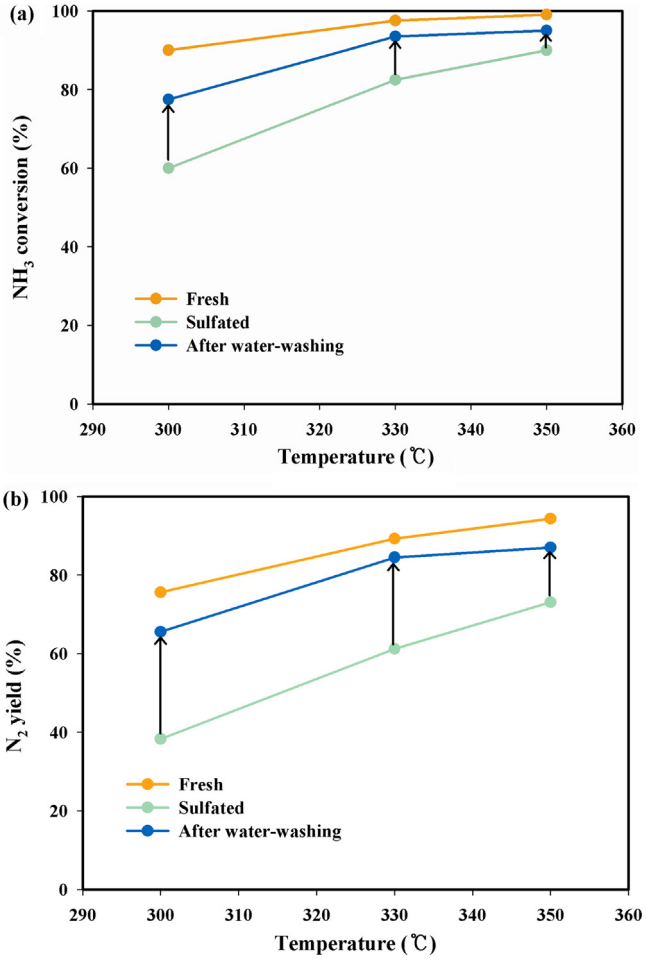

Fig. 8. NH_3 oxidation activities of fresh, sulfated and after water-washing over $10Ce/2V/TiO_2$ catalysts: (a) NH_3 conversion, (b) N_2 yield.

$2p_{3/2}$ are 464.4 and 458.8 eV, respectively, corresponding to typical Ti^{4+} oxidation state in a tetragonal structure [27]. Many researches show that as Ce impregnated the TiO_2, the binding energy of the Ti 2p peaks slightly shifted to higher binding energy than that of pure Ti 2p, because of the metal-support interaction effect generated by the addition of Ce atoms in TiO_2 support [19,36]. It is well known that these phenomena are much more affected by the Ce loadings, thermal treatment, or addition of another metal [37–41]. In this study, after the addition of Ce in TiO_2, the binding energies shifted slightly to higher values. With an addition of vanadium, the binding energies also exhibited higher value, than that of the $10Ce/TiO_2$ catalyst. This indicates that, when vanadium was impregnated, it had strong interaction with the TiO_2 support as shown in previous H_2 TPR results. The Gaussian fitting results of O 1s spectrums are shown in Fig. 5(c) It is well known that the O1s spectrum could be composed of three oxygen species. The first peak, which has a lower binding energy of 529.5–530.5 eV, is attributed to the lattice oxygen (O_α). The two overlapping peaks of O 1s with binding energies of 531.3–532 and 533–533.4 eV are attributed to surface adsorbed oxygen (O_β) and surface oxygen of hydroxyl species or adsorbed water species (O_γ), which were referred as in our previous paper [19]. With V doping, the chemisorbed surface oxygen (O_β) content was significantly increased. This is a promising result as the chemisorbed surface oxygen play an important role in the oxidation reaction, which had been reported by many studies [42,43]. The XPS analysis concluded that 2 wt% V doping in the $10Ce/TiO_2$ catalyst increased the Ce atoms (Ce^{4+} species) and surface oxygen and enhanced the SCO activity.

3.2.4. DRIFT study

To compare the reaction pathway between NO adspecies and $NH_3 + O_2$ for SCO reaction over $10Ce/TiO_2$ and $10Ce/2V/TiO_2$ catalysts, DRIFT studies were investigated, as shown in Fig. 6(a) and (b). Two catalysts were first treated with 5000 ppm NO at 350 °C for 30 min, and then NO was shut off, accompanied by 5000 ppm NH_3 + 8% O_2 injection, as a function of time. After NO adsorption on the $10Ce/TiO_2$ catalyst, the presence of adsorbed NO species were observed via bands at 1375 and 1490 cm^{-1}, which were assigned to the nitrate species [44]. Chen et al. [44] reported that the NO_x species were observed via bands at 1610, 1580, 1375 and 1240 cm^{-1} in the spectrum of Ce/Ti catalyst. Shan et al. [13] also reported that nitrate species bands ascribed to bridging nitrate (1625 and 1269 cm^{-1}), bidentrate nitrate (1603 cm^{-1}), and monodentate nitrate (1581 cm^{-1}) appeared. When only NO + O_2 were injected, these variations of NO_x species bands could be found. So, in this study, we only confirmed that two nitrate species bands were observed, due to just NO injection. The $10Ce/TiO_2$ catalyst

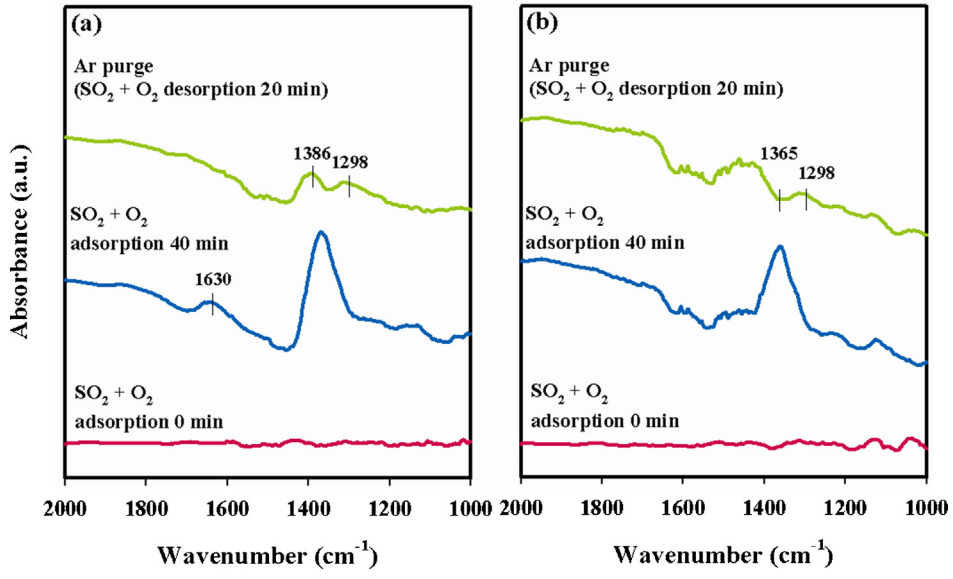

Fig. 9. DRIFT spectra of step reaction based on adsorption and desorption characteristics used SO_2, O_2 and Ar gas at 300 °C: (a) $10Ce/TiO_2$, (b) $10Ce/2V/TiO_2$.

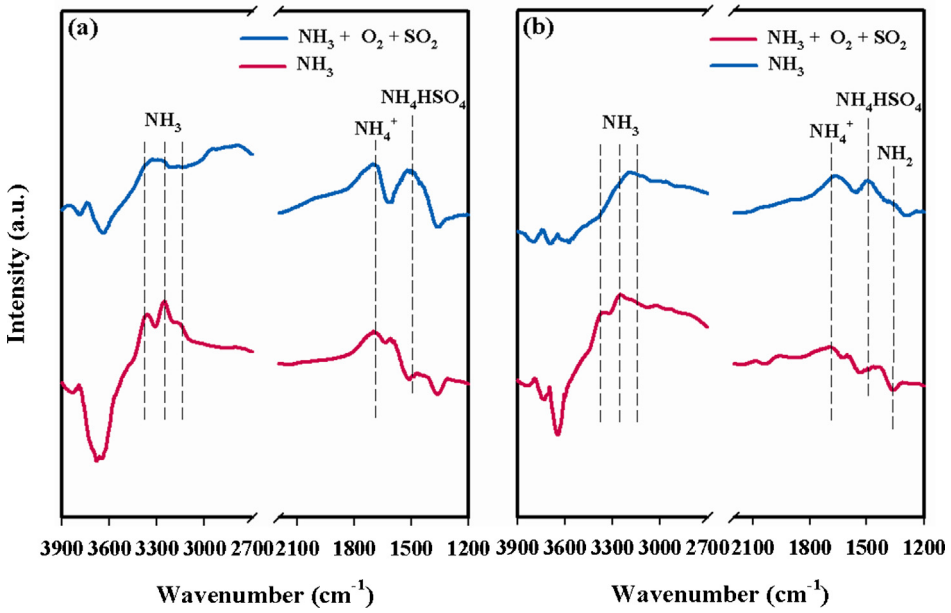

Fig. 10. DRIFT spectra of pre-adsorbed NH_3 reacted with "$SO_2 + O_2$" adsorption at 300 °C: (a) 10Ce/TiO_2, (b) 10Ce/2V/TiO_2.

was firstly injection with NO for 30 min, and then NO was shut off, accompanied by simultaneous $NH_3 + O_2$ introduction. The nitrate bands vanished, and a new band at 1551–1671 cm^{-1} appeared. After 20 min, new bands were observed at 1620 and 1321 cm^{-1}, which corresponded to the NO_2 and NH_2 bands, as shown in Fig. 6(a). This result indicates that the interaction of NH_3 with O_2 causes the formation of nitrates, and could continuously react with the adsorbed NH_3 or NH_2 species on the 10Ce/TiO_2 catalyst. In addition, adsorbed NH_2 can be readily oxidized to nitrates, which have been investigated in our previous studies. As compared to 10Ce/TiO_2 catalyst, the adsorbed NO bands on 10Ce/2V/TiO_2 catalyst showed a different trend. The adsorbed NO_x species were observed via bands at 1375 and 1620 cm^{-1}, which were assigned to the nitrate species and NO_2. The intensity of the bands assigned to nitrate species (1375 cm^{-1}) was higher, than that of 10Ce/TiO_2 catalyst. This means that the addition of vanadium to 10Ce/TiO_2 catalyst enhanced the adsorption of nitrate species at 350 °C, and the band at 1620 cm^{-1} due to adsorbed NO_x species transformed to other forms of NO_2 by abundant surface oxygen. NO_2 might be beneficial for continuous react with adsorbed NH_3 or NH_2 species, in good agreement with the literature [45]. When $NH_3 + O_2$ were introduced, the nitrate bands quickly vanished, and a band at 1551–1671 cm^{-1} was broadened. This may be due to two overlapping peaks between the NO_2 band at 1620 cm^{-1}, and stretching vibration of the NH_3 band on the Lewis acid sites at 1603 cm^{-1}. For 10Ce/2V/TiO_2 catalyst, the band of NH_2 at 1321 cm^{-1} showed a very similar trend on 10Ce/TiO_2 catalyst; whereas, the intensity of the band assigned to NH_2 at 1321 cm^{-1} was obviously higher, than that of 10Ce/TiO_2 catalyst. We also confirmed that the internal SCR pathway of NH_3 that follows a two-step mechanism, applies to the SCO reaction of NH_3 to N_2 on 10Ce/2V/TiO_2 catalysts. First of all, abundant adsorbed NH_2 species have a promoting effect on the formation of NO_x species, and this could accelerate the reaction with adsorbed NH_3 or NH_2 species and NO_x species over 10Ce/2V/TiO_2 catalyst. This is one possible reason why 10Ce/TiO_2 catalyst by vanadium addition showed higher SCO activity, than the 10Ce/TiO_2 catalyst.

3.3. *Effect of SO_2*

We investigated the influence of SO_2 on the catalytic activity of the 10Ce/TiO_2 and 10Ce/2V/TiO_2 catalysts, at a GHSV of 120,000 h^{-1}, in the temperature range of 300–350 °C. To evaluate the effect of SO_2 on the SCO reaction, 200 ppm SO_2 was fed for 5 h at each reaction temperature, which results are presented in Fig. 7. In the presence of SO_2, the NH_3 conversion was sharply decreased to 95% from 72.5%, and the N_2 yield was decreased to 68% from 79% over 10Ce/TiO_2 catalyst at 350 °C, as shown in Fig. 7(a). The 10Ce/TiO_2 catalyst is extremely deactivated by SO_2, and acts as a deactivator in the SCO reaction. These results suggest that the addition of SO_2 results in the formation of NH_4HSO_4 in the SCO reaction, which could deposit on the surface of the catalyst, and block the active sites [46]. While, the 10Ce/2V/TiO_2 catalyst showed the high catalytic activity, which achieved 90% conversion of NH_3, and 73% of N_2 yield at 350 °C, as shown in Fig. 7(b). Obviously, the resistance to SO_2 is attributed to the addition of vanadium in 10Ce/TiO_2 catalyst, and promoted the NH_3 conversion and N_2 yield, at all temperature regions.

SCO activities on fresh and sulfated 10Ce/2V/TiO_2 catalyst have been reported in Fig. 7. The used sulfated 10Ce/2V/TiO_2 catalysts were generated by filtering and washing with deionized water then dried at 103 °C overnight. Fig. 8(a) and (b) shows the SCO activities of fresh, sulfated and after water-washing over 10Ce/2V/TiO_2 catalyst. After water-washing of 10Ce/2V/TiO_2 catalyst, the NH_3 conversion was significantly recovered to 60% from 77.5%, and the N_2 yield was also recovered to 38.3% from 65.5% at 300 °C. It is well known that sulfate species deposit on catalyst surface of the active phase and the deposition of ammonium sulfate ($(NH_4)_2SO_4$) or ammonium bisulfate (NH_4HSO_4) in NH_3-SCR reaction [13,46,47]. In this study, these sulfated species deposited on 10Ce/2V/TiO_2 catalyst surface are mostly removed by water washing.

To investigate the SO_2 effect on the surface of 10Ce/TiO_2 and 10Ce/2V/TiO_2 catalysts for SCO reaction, DRIFT studies were performed. The catalysts were treated with 1000 ppm SO_2 with 8% O_2 adsorption at 300 °C for 40 min, and then purged by Ar for 20 min. After introducing $SO_2 + O_2$, three peaks centered at 1280, 1345–1475, and 1630 cm^{-1} were detected in 10Ce/TiO_2 catalyst (Fig. 9(a)); while one main peak at 1345–1475 cm^{-1} was observed in 10Ce/2V/TiO_2 catalyst (Fig. 9(b)). The broad band in the range of 1298 cm^{-1} was ascribed to bisulfate species, such as HSO^{4-} species. The band at 1345–1475 cm^{-1} was ascribed to O=S=O stretching frequency. Moreover, the band at 1630 cm^{-1} was assigned to adsorbed H_2O, due to the reaction of SO_2 and surface

hydroxyl groups [46]. In 10Ce/TiO_2 catalyst, the intensity of the band assigned to O=S=O stretching band (1345–1475 cm^{-1}) was higher, than that of 10Ce/2V/TiO_2 catalyst. After purge of Ar for 20 min, the intensities of SO_2 band attributed to 1345–1475 cm^{-1} (O=S=O stretching frequency) and 1298 cm^{-1} (HSO_4^- species) bands still remained in 10Ce/TiO_2 catalyst; whereas, the band at 1345–1475 cm^{-1} quickly vanished in 10Ce/2V/TiO_2 catalyst. This result indicated that the adsorbed SO_2 species were weakly bonded in 10Ce/2V/TiO_2 catalyst, and the lower thermal stability of the SO_2 species at 300 °C on 10Ce/2V/TiO_2 catalyst may lead to an increase in its sulfur tolerance.

Based on these results, we confirmed NH_4HSO_4 formation on the surface of catalyst, during the reaction between NH_3 and $SO_2 + O_2$. The catalysts were first adsorption with 5000 ppm NH_3 at 300 °C for 30 min, and then 1000 ppm SO_2 + 8% O_2 was fed for 30 min. The adsorption of NH_3 on Lewis acid sites was observed at 3253 cm^{-1} and 3364 cm^{-1}, and adsorption of NH_3 on Lewis acid sites was also observed at 3253 cm^{-1}, 3364 cm^{-1}, and 1603 cm^{-1}, which was a very similar trend on the two catalysts, as shown in Fig. 10(a) and (b). After introducing $SO_2 + O_2$, the intensity of the NH_3 bands decreased, and an NH_4^+ band at 1470 cm^{-1} appeared. This might be the reason SO_2 reacted with NH_3 to form NH_4HSO_4, which deposited on the catalyst surface, and did not decompose at 300 °C in the two catalysts. For 10Ce/2V/TiO_2 catalyst, the NH_4HSO_4 species peak also appeared, which was lower than for the 10Ce/TiO_2 catalyst. More importantly, the bands at 3253 cm^{-1} and 3364 cm^{-1}, which were attributed to coordinated NH_3, remained stable. A band of NH_2 at 1321 cm^{-1} very slightly appeared on 10Ce/2V/TiO_2 catalyst, in severe conditions (1000 ppm SO_2). We investigated the specific surface area of fresh and sulfated catalysts. The specific surface areas 10Ce/TiO_2 and 10Ce/2V/TiO_2 catalyst are significantly decreased from 74.48 to 58.65 m^2/g and 104.24 to 76.52 m^2/g due to the formation of NH_4HSO_4 on the surface of the catalyst. In future, mechanism studies of sulfur tolerance for the catalyst are one of the most important works for further research.

4. Conclusions

In this study, SCO activity results showed that the addition of vanadium on Ce/TiO_2 catalyst were greatly enhanced, which obtained 96% of NH_3 conversion with 90% N_2 yield over 10Ce/2V/TiO_2 catalyst, at the space velocity of 120,000 h^{-1}, at the temperature of 300 °C. From the XRD, TPR, XPS, and DRIFT studies, the results revealed that the addition of vanadium could result in better dispersion of Ce^{4+} species on TiO_2, and increased surface area, from 74.48 to 104.24 m^2/g. The vanadium also enhances the redox properties, which was beneficial to the SCO reaction. We confirmed that abundant adsorbed NH_2 species have a promoting effect on the formation of NO_x species, and it could accelerate the reaction with adsorbed NH_3 or NH_2 species and NO_x species, as an internal SCR mechanism over 10Ce/2V/TiO_2 catalyst. Finally, 10Ce/2V/TiO_2 catalyst showed strong resistance to SO_2 poisoning, which was beneficial for easy decomposition, in comparison with 10Ce/TiO_2 at 300 °C, in the presence of $NH_3 + SO_2 + O_2$. In summary, these results indicated that the 10Ce/2V/TiO_2 catalyst greatly improved the SCO activity and SO_2 tolerance.

Acknowledgement

This research was supported by the KIST Institutional Program (2E23900-13-021).

References

[1] G. Olofsson, A. Hinz, A. Andersson, Chem. Eng. Sci. 59 (2004) 4113–4123.
[2] S. Hong, A. Karim, T.S. Rahman, K. Jacobi, G. Ertl, J. Catal. 276 (2010) 371–381.
[3] M.J. Lippits, A.C. Gluhoi, B.E. Nieuwenhuys, Catal. Today 137 (2008) 446–452.
[4] Y. Li, J.N. Armor, Appl. Catal. B 13 (1997) 131–139.
[5] L. Zhang, H. He, J. Catal. 268 (2009) 18–25.
[6] L. Gang, J.V. Grondelle, B.G. Anderson, R.A.V. Santen, J. Catal. 186 (1999) 100–109.
[7] L. Chmielarz, P. Kustrowski, A.R. Lasocha, R. Dziembaj, Appl. Catal. B 58 (1997) 235–244.
[8] J.M.G. Amores, V.S. Escribano, G. Ramis, G. Busca, Appl. Catal. B 13 (1997) 45–58.
[9] L. Lietti, G. Ramis, G. Busca, F. Bregani, P. Forzatti, Catal. Today 61 (2000) 187–195.
[10] J.Y. Lee, S.B. Kim, S.C. Hong, Chemosphere 50 (2003) 1115–1122.
[11] Z. Wang, Z. Qu, X. Quan, H. Wang, Appl. Catal. A 411 (2012) 131–138.
[12] W. Shan, F. Liu, H. He, X. Shi, C. Zhang, Catal. Today 184 (2012) 160–165.
[13] W. Shan, F. Liu, H. He, X. Shi, C. Zhang, Appl. Catal. B 115–116 (2012) 100–106.
[14] Z. Wang, Z. Qu, X. Quan, Z. Li, H. Wang, R. Fan, Appl. Catal. B 134 (2013) 153–166.
[15] C. Liu, L. Chen, J. Li, L. Ma, H. Arandiyan, Y. Du, J. Xu, J. Hao, Environ. Sci. Technol. 46 (2012) 6182–6189.
[16] S.M. Lee, K.W. Park, S.C. Hong, Chem. Eng. J. 195 (2012) 323–331.
[17] P. Bazin, O. Saur, O. Marie, M. Daturi, J.C. Lavalley, A.M. Le Govic, V. Harlé, G. Blanchard, Appl. Catal. B 119 (2012) 207–216.
[18] S. Scire, C. Crisafulli, P.M. Riccobene, G. Patane, A. Pistone, Appl. Catal. A 417 (2012) 66–75.
[19] S.M. Lee, H.H. Lee, S.C. Hong, Appl. Catal. A 470 (2014) 189–198.
[20] G. Olofsson, R. Wallenberg, A. Andersson, J. Catal. 230 (2005) 1–13.
[21] W. Xu, H. He, Y. Yu, J. Phys. Chem. C 113 (2009) 4426–4432.
[22] R. Jin, Y. Liu, Z. Wu, H. Wang, T. Gu, Catal. Today 153 (2010) 84–89.
[23] Y. Shu, T. Aikebaier, X. Quan, S. Chen, H. Yu, Appl. Catal. B 150–151 (2014) 630–635.
[24] R.M. Yuan, G. Fu, X. Xu, H. Lin, J. Phys. Chem. C 115 (2011) 21218–21229.
[25] A. Moraes, M.H.M.T. Assumpcao, R. Papai, I. Gaubeur, R.S. Rocha, R.M. Reis, M.L. Calegaro, M.R.V. Lanza, M.C. Santos, J. Electroanal. Chem. 719 (2014) 127–132.
[26] N.M. Thuy, D.Q. Van, L.T.H. Hai, Nanomater. Nanotechnol. 2 (2012) 1–8.
[27] T. Gu, R. Jin, Y. Liu, H. Liu, X. Weng, Z. Wu, Appl. Catal. B 129 (2013) 30–38.
[28] P. Li, Y. Xin, Q. Li, Z. Wang, Z. Zhang, L. Zheng, Environ. Sci. Technol. 46 (2012) 9600–9605.
[29] G. Neri, A. Pistone, C. Milone, S. Galvagno, Appl. Catal. B 38 (2002) 321–329.
[30] S.M. Lee, S.S. Kim, S.C. Hong, Chem. Eng. Sci. 72 (2012) 177–185.
[31] S. Damyanova, C.A. Perez, M. Schmal, J.M.C. Bueno, Appl. Catal. A 234 (2002) 271–280.
[32] B. Murugan, A.V. Ramaswamy, J. Phys. Chem. C 112 (2008) 20429–20442.
[33] M.A. Banares, L.J. Alemany, M.C. Jimenez, M.A. Larrubia, F. Delgado, M.L. Granados, A.M. Arias, J.M. Blasco, H.L.G. Fierro, J. Solid State Chem. 124 (1996) 69–76.
[34] S. Watanabe, X. Ma, C. Song, J. Phys. Chem. C 113 (2009) 14249–14257.
[35] F. Zhang, P. Wang, J. Koberstein, S. Khalid, S.W. Chan, Surf. Sci. 563 (2004) 74–82.
[36] L. Chen, J. Li, M. Ge, J. Phys. Chem. C 113 (2009) 21177–21184.
[37] J. Fang, X. Bi, D. Si, Z. Jiang, W. Huang, Appl. Surf. Sci. 253 (2007) 8952–8961.
[38] J. Petryk, E. Kolakowska, Appl. Catal. B 24 (2000) 121–128.
[39] M. Luo, J. Chen, L. Chen, L. Lu, Z. Feng, C. Li, Chem. Mater. 13 (2001) 197–202.
[40] S. Yang, W. Zhu, Z. Jiang, Z. Chen, J. Wang, Appl. Surf. Sci. 252 (2006) 8499–8505.
[41] M. Suzana, P. Francisco, V.R. Mastelaro, Chem. Mater. 14 (2002) 2514–2518.
[42] B. Shen, Y. Wang, F. Wang, T. Liu, Chem. Eng. J. 236 (2014) 171–180.
[43] Z. Wu, R. Jin, Y. Liu, H. Wang, Catal. Commun. 9 (2008) 2217–2220.
[44] L. Chen, J. Li, M. Ge, Environ. Sci. Technol. 44 (2010) 9590–9596.
[45] M. Koebel, G. Madia, F. Raimondi, A. Wokaun, J. Catal. 209 (2002) 159–165.
[46] R. Jin, Y. Liu, Y. Wang, W. Cen, Z. Wu, H. Wang, X. Weng, Appl. Catal. B 148–149 (2014) 582–588.
[47] J. Huang, Z. Tong, Y. Huang, J. Zhang, Appl. Catal. B 78 (2008) 309–314.